The International Archives of the Photogrammetry, Remote Sensing and Spatial Information Sciences, Volume XLVIII-2/W3-2023
ISPRS Intl. Workshop “Photogrammetric and computer vision techniques for environmental and infraStructure monitoring, Biometrics and Biomedicine”
PSBB23, 24–26 April 2023, Moscow, Russia

MULTI-CLASS SEGMENTATION OF HETEROGENEOUS AREAS IN BIOMEDICAL AND ENVIRONMENTAL IMAGES BASED ON THE ASSESSMENT OF LOCAL EDGE DENSITY

A. M. Sinitca[1], A. I. Lyanova[1]*, D. I. Kaplun[1], P. V. Zelenikhin[2], R. G. Imaev[3],
A. M. Gafurov[3], B. M. Usmanov[3], D. V. Tishin[3], A. R. Kayumov [2], M. I. Bogachev[1]

[1] Centre for Digital Telecommunication Technologies, St. Petersburg Electrotechnical University “LETI”,
197022, 5 Professor Popov street, St. Petersburg, Russia - amsinitca@etu.ru, rogex@yandex.ru

[2] Institute for Fundamental Medicine and Biology, Kazan Federal University,
420008, 18 Kremlevskaya street, Kazan, Tatarstan, Russia – kairatr@yandex.ru

[3] Institute of Environmental Sciences, Kazan Federal University,
420008, 18 Kremlevskaya street, Kazan, Tatarstan, Russia – kpfuecology@gmail.com

Commission II, WG II/8

KEY WORDS: multispectral images, remote sensing, segmentation, patchiness, edge density

ABSTRACT:

Imaging techniques employed in biomedical and ecological applications typically require complex equipment and experimental approaches, including sophisticated multispectral cameras, as well as physical markup of samples, altogether limiting their broad availability. Accordingly, computerized methods allowing to obtain similar information from images obtained in visible light spectrum with reasonable accuracy are of considerable interest. Edge detection methods are commonly used to find discriminating curves in image segmentation. Here we follow an alternative route and employ edge detection results as a separate metric characterizing local structural properties of the image. In turn, their characteristics such as density or orientation averaged in a gliding window are used as a virtual channel substituting multispectral imaging and/or physical markup of samples, and the following image segmentation procedures are performed by thresholding. In complex segmentation scenarios, a single fixed threshold often appears sufficient, and thus relevant adaptive multi-threshold algorithms are of interest, with slope difference distribution (SDD) thresholding algorithm representing a prominent example.

1. INTRODUCTION

Quantitative image analysis represent a challenging problem for a variety of biomedical investigations, ecological monitoring and clinical applications. Prominent examples can be found in microscopy data analysis, such as *in vitro* cell growth and migration, histology, wound healing and many others. Another prominent application area includes remote sensing images widely used in ecological monitoring, typically obtained using either local UAV observations or global satellite data.

Image segmentation in biomedical applications is generally based either on physical procedures such as differential fluorescent staining common in microscopic imaging, use of contrast agents in X-ray tomography or radiotracing in positron-emission tomography, respectively, as well as computer vision approaches. In remote sensing images, segmentation is typically focused on the analysis of multispectral images, typically represented by geological or vegetation indices calculated from the relative intensities in several frequency bands. In certain designs, the above approaches can be combined leading to multispectral imaging of objects that underwent preliminary physical markup procedures.

Applying above techniques typically requires sophisticated equipment, as well as preparatory staining or contrasting procedures where applicable, that imposes inevitable limitations to their applicability. Accordingly, computerized segmentation of visual (bright-field) images is of considerable interest in a number of applications where physical staining or contrasting, as well as multispectral imaging is either unavailable or economically unfeasible.

Simple computer vision methods such as intensity thresholding are typically efficient only in combination with physical markup based either on staining or contrasting of studied samples, a common approach in microscopic imaging in various biomedical research settings, or on the calculation of specialized indices based on multiple spectral bands, a common approach in remote sensing with multiple applications in agricultural, geological and other environmental sciences (Bogachev et al., 2018, Bogachev et al., 2019, Volkov et al., 2020). Therefore, in recent years deep learning based solutions attracted considerable attention due to their potentially higher accuracy, although at the cost of performance and resource intensiveness.

However, their major drawback is the requirement of extensive learning procedures based on large reference image sets that are well beyond common sizes of biomedical and ecological images originating from single studies. While large image bases are becoming increasingly available and representative, it is always questionable to which extent are they representative in the context of particular studies, and relevant subselections represent a separate issue.

Altogether, the above limitations remain the common drivers of continuous interest in more general and universal computer vision methods suitable for various scenarios where using ad-

* Corresponding author

Table 1. Spectral channels used in remote sensing analysis.

Channel	Center $\pm$ bandwidth, nm
BLUE	475 ± 32
GREEN	560 ± 27
RED	668 ± 16
Red edge (RE)	717 ± 12
Near infrared (NIR)	842 ± 57

vanced deep learning methods is unfeasible due to the lack of available image sets for learning procedures, as well as limited computational resources.

Patchiness is a ubiquitous structural property that could be observed in almost any natural and especially biological system. Prominent examples range from cell cultures and tissues to plants and animal motion patterns, just to mention a couple of prominent examples (Sinitca et al., 2023, Bogachev et al., 2023a, Bogachev et al., 2023b). In a recent work, we have suggested a simple algorithm for a semi-automatic segmentation and quantification of patchy areas in biomedical images considering the local edge density as a quantitative metric of patchiness (Sinitca et al., 2023). The proposed algorithm has been implemented in a simple open-source software tool with only a couple of tuning parameters controllable online with immediate visualization of the results this way allowing for a straightforward domain-expert feedback available at (Sinitca, 2023a).

2. MATERIALS AND METHODS

2.1 Multi-spectral remote sensing images

Next, we analyzed images obtained by remote sensing observations of a local area containing a patchy landscape pattern, including a fragment of a river, a river bank, a local part of a planted conifer forest, and a part of a field involved in regular agricultural activities. Remote sensing imagery has been acquired using Geoscan 401 Geodesy UAV equipped with a MicaSense RedEdge-MX (RX02 series) multi-spectral camera (pixel size $3.75\mu m$, resolution 1280×960 (1.2 MP $\times 5$ imagers), aspect ratio 4:3, sensor size 4.8 mm $\times 3.6$ mm, focal length 5.4 mm, field of view: 47.2 degrees horizontal, 35.4 degrees vertical, output depth 12 bit). The recorded channels are outlined in the Table 1.

A brief summary of the multi-spectral vegetation indices (Tucker, 1979, Rondeaux et al., 1996, Jiang et al., 2008, Gitelson and Merzlyak, 1998, Schuster et al., 2012) considered in this study is outlined below.

- **Chlorophyll Index - Green (CIg)**. Vegetation index for estimating the chlorophyll content in leaves using the ratio of reflectivity in the NIR and green bands.

$$CIg = \frac{NIR}{GREEN} - 1 \tag{1}$$

- **Burn Area Index (BAI)**. Uses the reflectance values in the red and NIR portion of the spectrum to identify the areas of the terrain affected by fire.

$$BAI = \frac{1}{(0.1 - RED)^2 + (0.06 - NIR)^2} \tag{2}$$

- **Enhanced Vegetation Index (EVI)**. An optimized vegetation index that accounts for atmospheric influences and vegetation background signal. It's similar to NDVI but is less sensitive to background and atmospheric noise, and it does not become as saturated as NDVI when viewing areas with very dense green vegetation.

$$EVI = \frac{2.5(NIR - RED)}{NIR + 6RED - 7.5BLUE + 1} \tag{3}$$

- **Green Normalized Difference Vegetation Index (GNDVI)**. Vegetation index for estimating photo synthetic activity and is a commonly used vegetation index to determine water and nitrogen uptake into the plant canopy.

$$GNDVI = \frac{NIR - GREEN}{NIR + GREEN} \tag{4}$$

- **Normalized Difference Vegetation Index (NDVI)**. Standardized index allowing you to generate an image displaying greenness (relative biomass). This index takes advantage of the contrast of the characteristics of two bands from a multispectral raster dataset – the chlorophyll pigment absorptions in the red band and the high reflectivity of plant materials in the NIR band.

$$NDVI = \frac{NIR - RED}{NIR + RED} \tag{5}$$

- **Iron Oxide (IO) ratio**. A geological index for identifying rock features that have experienced oxidation of iron-bearing sulfides using the red and blue bands. IO is useful in identifying iron oxide features below vegetation canopies and is used in mineral composite mapping.

$$IO = \frac{RED}{BLUE} \tag{6}$$

- **Red-Edge Triangulated Vegetation Index (RTVICore)**. Vegetation index for estimating leaf area index and biomass. This index uses reflectance in the NIR, red-edge, and green spectral bands.

$$RTVICore = 100(NIR - RE) - 10(NIR - GREEN) \tag{7}$$

- **Simple Ratio (SR)**. A common vegetation index for estimating the amount of vegetation. It is the ratio of light scattered in the NIR and absorbed in red bands, which reduces the effects of atmosphere and topography.

$$SR = \frac{NIR}{RED} \tag{8}$$

- **Visible Atmospherically Resistant Index (VARI)**. A vegetation index for estimating vegetation fraction quantitatively with only the visible range of the spectrum.

$$VARI = \frac{GREEN - RED}{GREEN + RED - BLUE} \tag{9}$$

- **Modified Triangular Vegetation Index (MTVI2)**. Vegetation index for detecting leaf chlorophyll content at the canopy scale while being relatively insensitive to leaf area

index. It uses reflectance in the green, red, and NIR bands.

$$MTVI2 = 1.5(1.2(NIR - GREEN)) - \\ - 2.5(RED - GREEN) \times \\ \times \sqrt{(2NIR + 1)^2 - (6NIR - 5\sqrt{RED}) - 0.5} \quad (10)$$

To evaluate whether the proposed virtual local edge density channel carries significant information about the geophysical characteristics and vegetation conditions in the observed area, we performed regression analysis to evaluate the relationship between the local edge densities and the above geological and vegetation indices. The accuracy of the regression models has been estimated using both the linear Pearson's and the non-parameteric (rank) Spearman's correlation coefficients. The higher are the respective correlation coefficients, a potentially better prediction of the respective multi-spectral index from the virtual local edge density channel could be obtained by using the best linear and non-linear fits, respectively.

2.2 Microscopic images

To validate the proposed approach, we first consider a recently reported image set containing human colon adenocarcinoma Caco-2 cells microscopy images obtained in both bright-field and fluorescent regimes (Trizna et al., 2023). In the following, we analyze the respective image series using the edge density based segmentation algorithm. First, we extract the local edge densities from the bright-field microscopy images to create a virtually "stained" channel. In the following, for image segmentation we apply either the conventional Otsu thresholding reproducing the algorithm recently proposed in (Sinitca et al., 2023), or the slope difference distribution (SDD) multi-thres-holding algorithm based on a recently proposed multi-thresholding methodology (Wang, 2016). While we remain focused on the binary classification scenario, we test three different threshold values derived from SDD denoted as the lower, median and upper thresholds, and evaluate the segmentation accuracy for each of them.

2.3 Patchiness estimation and segmentation

The proposed approach is a generalization of our recent development originally reported in (Sinitca et al., 2023) for the semi-automated segmentation of biomedical images according to their patchiness based on local edge density estimation. In contrast to this recent work, which focused solely on binary segmentation using Otsu thresholding in the final step of the algorithm, in the current study we generalize the thresholding procedure by considering a multi-class segmentation scenario using a different approach for quantization. Thus, in the final step of the algorithm the image segmentation is performed by a more advanced alternative based on the slope difference distribution (SDD) (Wang, 2016). Among recent approaches to the automated thresholding problem, a slope difference distribution (SDD) based approach (Wang, 2016) seems to at least partially overcome the common limitations of conventional thresholding methods, including promising evidence from medical imaging applications (Wang, 2020). One important feature of the above algorithm is the embedded opportunity of multi-thresholding based on the data-driven estimates of the threshold values.

3. RESULTS

3.1 Analysis of remote sensing data

Images representing five spectral bands and ten multispectral indices as summarized in subsection 2.1 for the analyzed area are shown in Fig. 1. The figure shows that there are several areas with prominent contrast between them altogether observed in several channels and indices, in particular, (A) the river and the adjusted river bank in the upper right part of the image, (B) a forested area in the central part of the image, as well as (C) a field area characterized by continuous agricultural activities in the lower left part of the image. The figure shows that most of the considered indices indicate major contrast between these areas, with just a few exceptions.

In the following, we test whether the respective geological and vegetation indices could be effectively predicted based on the local edge density estimates. For that, we performed regression analysis of the local edge densities on ten studied indices outlined above. Three regression models characterized by the highest linear Pearson's and non-parameteric Spearman's correlation coefficients, among them are the commonly used vegetation index $GNDVI$, the burned area index BAI typically used to detect traces of forest fires, as well as the geological index IO reflecting traces of oxidation on the ground, are exemplified in Fig. 2. Based on the results of the regression analysis, the above indices could be presumably predicted from the virtual local edge density channel calculated solely from visible light observations, representing a kind of low-cost alternative to multispectral imaging, at least in a rough approximation.

In the following, we analyzed whether the observed contrast could be used for the image segmentation according to local land cover and use characteristics. Figure 3 represents prominent examples of multi-class segmentation procedures based on the adaptive thresholding based on the slope difference distribution (SDD), according to (Wang, 2016). Figure 3 shows the multispectral indices and the local edge densities (as denoted in the respective panel caption), as well as intensity distributions for the respective index channels with bin edges provided by the multi-class segmentation algorithm indicated by vertical dashed lines, and finally segmentation results with classes denotes by color.

Of note, the proposed approach exhibits lower effective resolution, since the local properties are estimated via the region features. To match with the edge density resolution, we have also reduced the effective resolution of the multi-spectral bands, as well as geological and vegetation indices prior to the correlation analysis using the Windowed Moving Average Filter.

3.2 Cells segmentation

Figure 4 exemplifies the results of multi-level cells segmentation performed using the edge density estimation procedure followed by automated thresholding using the algorithm originally proposed in (Wang, 2016). The figure shows that cells and cell clumps are being successfully distinguished from the image background using local edge density, that does not require any physical markup like contrasting or staining. In comparison with the recently reported algorithm (Sinitca et al., 2023), using multi-thresholding opens ways towards multi-class segmentation that is essential in a variety of experimental settings, for example, when specified cells sub-populations have to be distinguished and selected (see, e.g., (Bogachev et al., 2018, Bogachev et al., 2019, Volkov et al., 2020) and references therein).

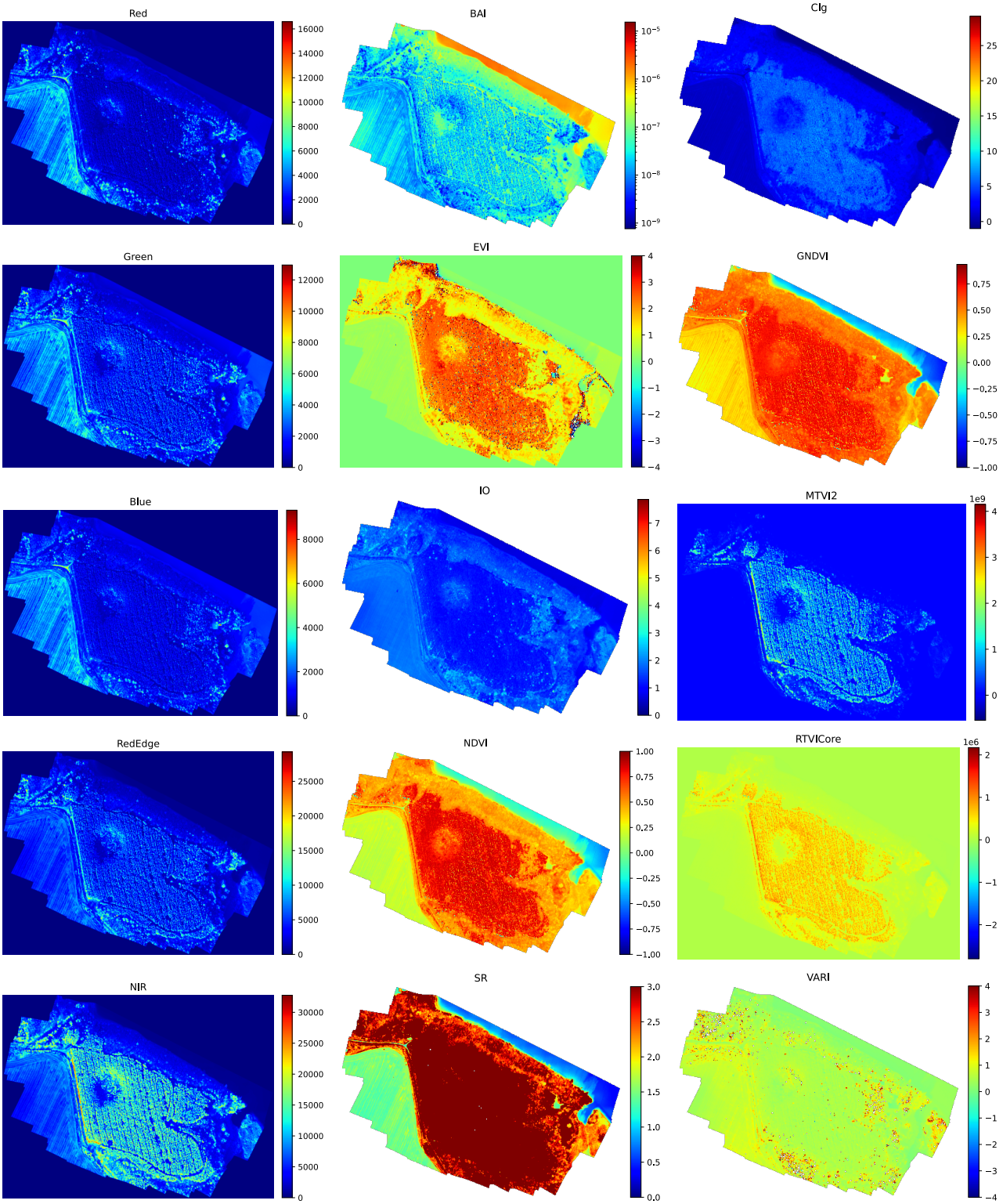

Figure 1. Five-band images (Red, Green, Blue, Red-Edge, Near-Infrared) obtained by multispectral remote sensing (left column), as well as ten different multispectral geological and vegetation indices (central and right columns, respectively).

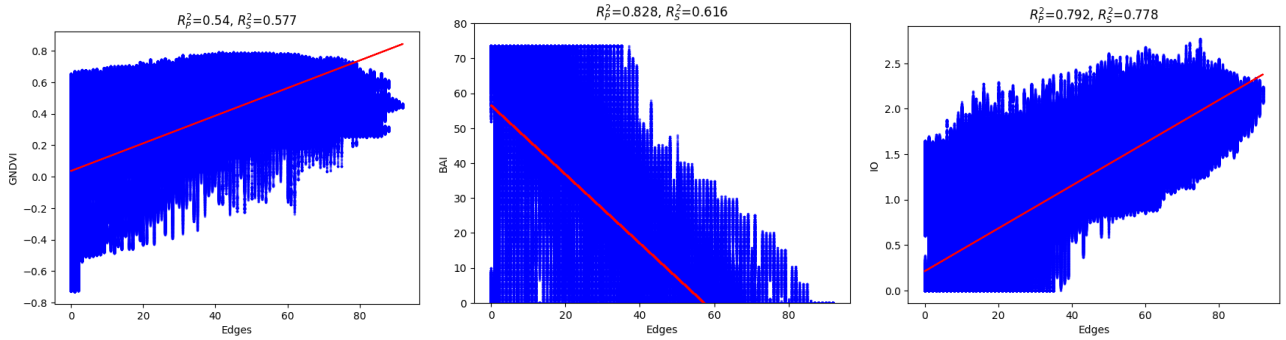

Figure 2. Linear regression analysis between multispectral vegetation and geological indices (GNDVI, BAI, and IO) and edge density providing a surrogate channel obtained solely from visible light image analysis. Pearson’s and Spearman’s correlations are indicated in the panel subtitles.

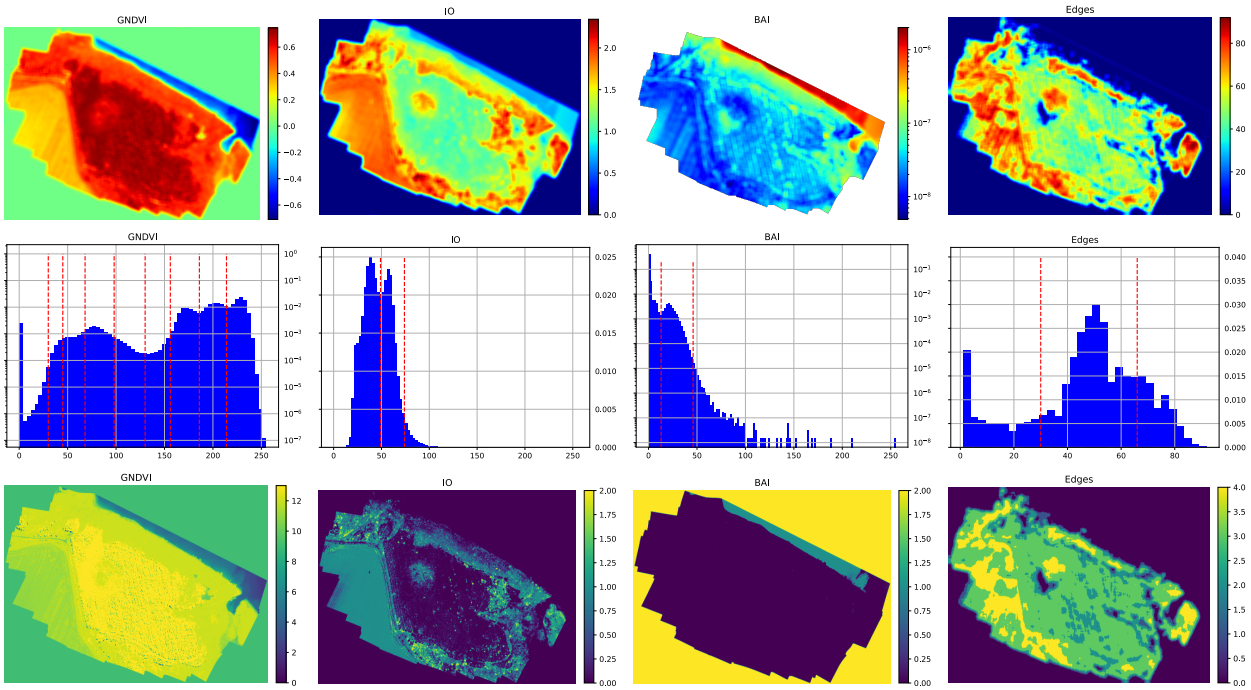

Figure 3. Top to bottom: multispectral indices and local edge densities (as denoted in the respective panel captions); intensity distributions for the respective index channels with bin edges provided by the multi-class segmentation algorithm indicated by vertical dashed lines; segmentation results with classes denoted by color.

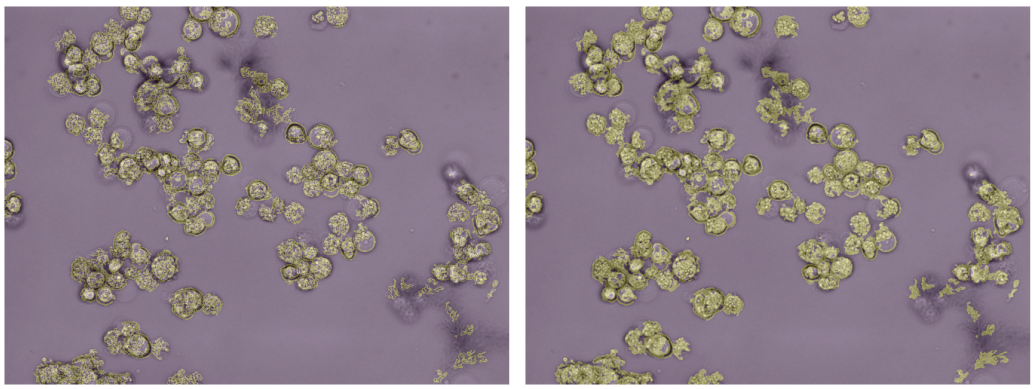

Figure 4. Example of cells multilevel segmentation. The left panel shows the segmentation at the lower threshold provided by the SDD algorithm, while the right one shows similar results for the upper threshold, respectively.

4. CONCLUSION

To summarize, we have shown explicitly that the local edge density estimate represents a perspective tool for the structural characterization of the local image content. In some cases, this virtual markup could be used to predict certain local image features without relying upon sophisticated physical contrasting or staining, as well as using high-tech multi-spectral equipment, and thus also reducing associated laboratory costs. In contrast to the recently proposed solution for the binary classification scenario (Sinitca et al., 2023), in this work by combining the edge density estimation with the SDD based thresholding, we have suggested a route towards multi-class segmentation based on the local structural properties. Our results indicate that the proposed methodology is capable of discriminating between several classes in remote sensing images, such as water surface (river), forest, and field, and thus could be employed for a rough evaluation based on visible light images only, reducing the costs for advanced multispectral equipment, as well as avoiding the use of any physical markup technologies.

Among certain limitations of the present implementation, we like to note that the SDD algorithm may be unstable when significant part of the image histogram appears empty. In this case, redundant thresholds may appear, leading to periodic binning in the tail of the distribution. Accordingly, in some cases further corrections, including elimination of these redundant bin edges, are required. Although these procedures could be automated as well, in many practical applications semi-automatic analysis with expert control over the number of bins, and thus also the number of bin edges, would likely be of interest.

Finally, we have implemented the proposed segmentation algorithm in a simple open-source software tool with on-the-fly visualization for straightforward feedback by a domain expert that does not require any specific experience in image analysis techniques. The software tool and the image sets used in the above analysis and algorithm validation are freely available online at (Sinitca, 2023a).

Additionally, we have implemented in Python the slope difference distribution (SDD) algorithm. The library is freely available online at (Sinitca, 2023b).

ACKNOWLEDGEMENTS

We would like to acknowledge the support of this work by the Russian Science Foundation (project No. 22-76-10042), `https://rscf.ru/project/22-76-10042/`.

REFERENCES

Bogachev, M. I., Lyanova, A. I., Sinitca, A. M., Pyko, S. A., Pyko, N. S., Kuzmenko, A. V., Romanov, S. A., Brikova, O. I., Tsygankova, M., Ivkin, D. Y. et al., 2023a. Understanding the complex interplay of persistent and antipersistent regimes in animal movement trajectories as a prominent characteristic of their behavioral pattern profiles: Towards an automated and robust model based quantification of anxiety test data. *Biomedical Signal Processing and Control*, 81, 104409.

Bogachev, M. I., Volkov, V. Y., Kolaev, G., Chernova, L., Vishnyakov, I., Kayumov, A., 2019. Selection and quantification of objects in microscopic images: from multi-criteria to multi-threshold analysis. *Bionanoscience*, 9(1), 59–65.

Bogachev, M. I., Volkov, V. Y., Markelov, O. A., Trizna, E. Y., Baydamshina, D. R., Melnikov, V., Murtazina, R. R., Zelenikhin, P. V., Sharafutdinov, I. S., Kayumov, A. R., 2018. Fast and simple tool for the quantification of biofilm-embedded cells sub-populations from fluorescent microscopic images. *PLOS ONE*, 13(5), 1-24.

Bogachev, M., Sinitca, A., Grigarevichius, K., Pyko, N., Lyanova, A., Tsygankova, M., Davletshin, E., Petrov, K., Ageeva, T., Pyko, S. et al., 2023b. Video-based marker-free tracking and multi-scale analysis of mouse locomotor activity and behavioral aspects in an open field arena: A perspective approach to the quantification of complex gait disturbances associated with Alzheimer's disease. *Frontiers in Neuroinformatics*, 17, 1101112.

Gitelson, A. A., Merzlyak, M. N., 1998. Remote sensing of chlorophyll concentration in higher plant leaves. *Advances in Space Research*, 22(5), 689–692.

Jiang, Z., Huete, A. R., Didan, K., Miura, T., 2008. Development of a two-band enhanced vegetation index without a blue band. *Remote sensing of Environment*, 112(10), 3833–3845.

Rondeaux, G., Steven, M., Baret, F., 1996. Optimization of soil-adjusted vegetation indices. *Remote sensing of environment*, 55(2), 95–107.

Schuster, C., Förster, M., Kleinschmit, B., 2012. Testing the red edge channel for improving land-use classifications based on high-resolution multi-spectral satellite data. *International Journal of Remote Sensing*, 33(17), 5583–5599.

Sinitca, A. M., 2023a. BCAnalyzer. https://gitlab.com/digiratory/biomedimaging/bcanalyzer.

Sinitca, A. M., 2023b. Slope Difference Distribution Segmentation. https://gitlab.com/digiratory/sdd-segmentation.

Sinitca, A. M., Kayumov, A. R., Zelenikhin, P. V., Porfiriev, A. G., Kaplun, D. I., Bogachev, M. I., 2023. Segmentation of patchy areas in biomedical images based on local edge density estimation. *Biomedical Signal Processing and Control*, 79, 104189.

Trizna, E., Sinitca, A., Lyanova, A., Baidamshina, D., Zelenikhin, P., Kaplun, D., Kayumov, A., Bogachev, M., 2023. Brightfield vs Fluorescent Staining Dataset - A Test Bed Image Set for Machine Learning based Virtual Staining. *Scientific Data*, 10, https://doi.org/10.1038/s41597-023-02065-7.

Tucker, C. J., 1979. Red and photographic infrared linear combinations for monitoring vegetation. *Remote sensing of Environment*, 8(2), 127–150.

Volkov, V. Y., Bogachev, M. I., Kayumov, A. R., 2020. Object selection in computer vision: from multi-thresholding to percolation based scene representation. *Computer Vision in Advanced Control Systems-5*, Springer, 161–194.

Wang, Z., 2016. A new approach for segmentation and quantification of cells or nanoparticles. *IEEE Transactions on Industrial Informatics*, 12(3), 962–971.

Wang, Z., 2020. Automatic localization and segmentation of the ventricles in magnetic resonance images. *IEEE Transactions on Circuits and Systems for Video Technology*, 31(2), 621–631.